



Article

Mechanisms Underlying Antipsychotic-Induced NAFLD and Iron Dysregulation: A Multi-Omic Approach

Meghan May *, Deborah Barlow, Radwa Ibrahim and Karen L. Houseknecht *

Department of Biomedical Sciences, College of Osteopathic Medicine, University of New England, Biddeford, ME 04005, USA; dbarlow@une.edu (D.B.); ribrahim1@une.edu (R.I.)

* Correspondence: mmay3@une.edu (M.M.); khouseknecht@une.edu (K.L.H.); Tel.: +1-207-602-2872 (K.L.H.)

Abstract: Atypical antipsychotic (AA) medications are widely prescribed for the treatment of psychiatric disorders, including schizophrenia, bipolar disorder and treatment-resistant depression. AA are associated with myriad metabolic and endocrine side effects, including systemic inflammation, weight gain, dyslipidemia and insulin resistance, all of which are associated with increased incidence of non-alcoholic fatty liver disease (NAFLD). NAFLD is highly prevalent in patients with mental illness, and AA have been shown to increase incidence of NAFLD pre-clinically and clinically. However, the underlying mechanisms have not been described. We mined multi-omic datasets from preclinical murine models of sub-chronic risperidone or olanzapine treatment, in vitro exposure of human cells to risperidone and psychiatric patients following onset of aripiprazole therapy focused on pathways associated with the pathophysiology of NAFLD, including iron accumulation, systemic inflammation and dyslipidemia. We identified numerous differentially expressed traits affecting these pathways conserved across study systems and AA medications. We used these findings to propose mechanisms for AA-associated development of NAFLD and dysregulated iron homeostasis.



Citation: May, M.; Barlow, D.; Ibrahim, R.; Houseknecht, K.L. Mechanisms Underlying Antipsychotic-Induced NAFLD and Iron Dysregulation: A Multi-Omic Approach. *Biomedicines* **2022**, *10*, 1225. <https://doi.org/10.3390/biomedicines10061225>

Academic Editors: François R. Jornayvaz and Karim Gariani

Received: 1 March 2022

Accepted: 19 May 2022

Published: 24 May 2022

Publisher's Note: MDPI stays neutral with regard to jurisdictional claims in published maps and institutional affiliations.



Copyright: © 2022 by the authors. Licensee MDPI, Basel, Switzerland. This article is an open access article distributed under the terms and conditions of the Creative Commons Attribution (CC BY) license (<https://creativecommons.org/licenses/by/4.0/>).

Keywords: NAFLD; NASH; antipsychotic; inflammation; insulin resistance; iron metabolism; anemia; psychiatry

1. Introduction

Non-alcoholic fatty liver disease (NAFLD) is the most common cause of liver disease in the world and is characterized by the presence of steatosis in >5% of hepatocytes by histological analysis [1]. It has a prevalence rate of up to 25–30% in the general population with an upwards trend. Non-alcoholic steatohepatitis (NASH) represents advanced-stage disease progression, leading to cirrhosis and ultimately liver failure, making NASH one of the leading indications for liver transplantation [2]. NAFLD, the hepatic manifestation of insulin resistance and metabolic syndrome, is highly comorbid with obesity, and is considered an independent risk factor for cardiovascular disease [3,4]. Furthermore, growing evidence supports an association between metabolic syndrome and psychiatric disorders, such as schizophrenia, bipolar disorder and depression [5]. A recent study examining psychiatric patients without prior liver-related events found that liver disease was the fifth most common cause of death in this population [6]. Myriad factors likely contribute to increased NAFLD incidence in patients with mental illness, including the effects of psychiatric medications such as antipsychotic drugs [6–8]. Antipsychotic medications have complex and diverse pharmacology and are prescribed for myriad indications including schizophrenia, bipolar disorder, treatment resistant depression and irritability associated with autism [9]. These drugs are associated with significant endocrine, metabolic and inflammatory side effects including insulin resistance, dyslipidemia and NAFLD, and drug effects are distinct from metabolic side effects associated with psychiatric illness [10,11]. Rapid weight gain is a common occurrence in first-episode psychosis treated with AA medications [12–14], and the majority of patients have persistent body mass indices (BMI)

classified as obese [15]. We and others have reported that clinically relevant exposures of the atypical antipsychotic (AA) medications risperidone and olanzapine induced histologically confirmed NAFLD with coincident alteration in proteomic signatures consistent with insulin resistance, dysregulated inflammation and mitochondrial dysfunction in pre-clinical models [7,9,16,17].

Development of NAFLD is complex and multifaceted (Figure 1), and some of the underlying pathophysiological mechanisms are not well understood. One such mechanism is the relationship between NAFLD and iron homeostasis. Patients with NAFLD often present with alterations in iron metabolism, and there is an increase in hepatic iron stores in about one third of patients with NAFLD [18,19].

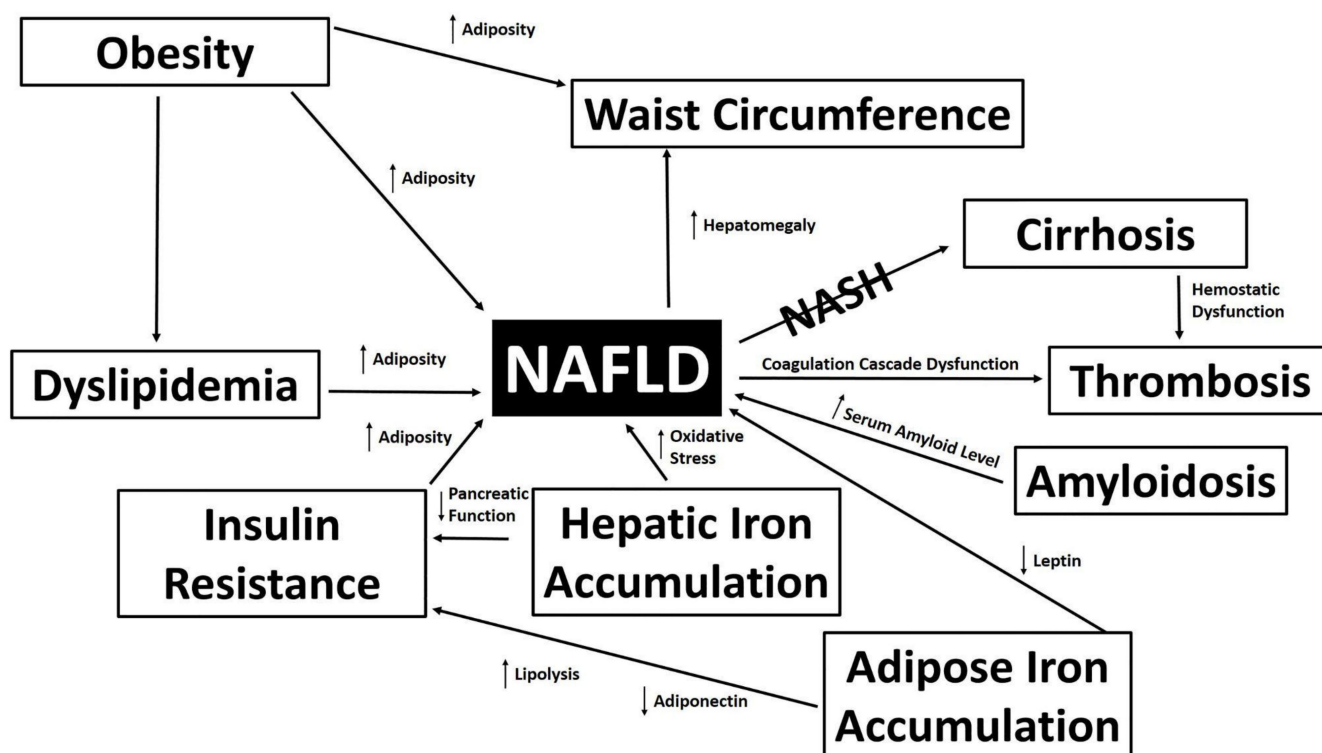


Figure 1. The Pathophysiology of NAFLD. Clinical states and changing metrics associated with NAFLD are depicted.

Dysregulation of iron metabolism is associated with cognitive disorders, including memory and attention disorders, with or without anemia [20–22]. Although the molecular mechanisms are not well defined, iron overload induces insulin resistance and increases oxidative stress, which in turn leads to further alteration in insulin signaling pathways and fat metabolism [23]. Antipsychotic medications can also disrupt iron metabolism, leading to akathisia and hypoferritinemia/iron-deficiency anemia, particularly in pediatric patients [24–26].

The association of NAFLD with disrupted iron homeostasis, coupled with the induction of both states by AA medications, suggests a complex, interdependent relationship between AA-induced NAFLD and dysregulated iron metabolism. In this study we used a multi-omic translational approach to evaluate AA-induced changes in pathways linked to NAFLD and iron metabolism. We identified differentially expressed (DE) traits conserved across study systems including three AA medications and three treatment modalities and used these findings to propose pathophysiological mechanisms of AA-induced NAFLD with disrupted iron homeostasis.

2. Materials and Methods

2.1. Proteomic and Immunomic Changes Induced by Risperidone and Olanzapine in Non-Obese Mice

Hepatic and cardiac proteomes and serum immunomes from young adult C57BL/6 J mice were measured following oral treatment with risperidone (RIS, 1 mg/kg), olanzapine (OLAN, 5 mg/kg) or a drug vehicle (VEH, 0.1% acetic acid) for 4 weeks as previously described [9,16]. Briefly, 8-week-old male mice were fed a standard, low-fat chow diet for the duration of the study (28 days) and treated with RIS and OLAN doses, whose peak plasma drug concentrations fall within the range of plasma drug exposures observed clinically in patients. Hepatic and cardiac proteomes were determined by mass spectrometry and profiled by sequential window acquisition of all theoretical spectra (SWATH) analysis [16]. Serum immunomes were determined using the Proteome Profiler Mouse Cytokine Array (R&D Systems, Minneapolis, MN, USA). Differentially expressed (DE) proteins were identified by Student's *t* test using a significance cutoff of $p < 0.05$. The proteomic datasets analyzed for this study can be found in the PeptideAtlas (identifier: PASS01349) <http://www.peptideatlas.org/PASS/PASS01349> (Access date 20 January 2022). There were no significant changes in animal body weight, and NAFLD in AA-treated animals was histologically confirmed [7,9,16].

2.2. Transcriptomic Changes Induced by Risperidone Treatment of Human Neuroblastoma Cells In Vitro

Transcriptomes from low passage human neuroblastoma cells incubated in 24 h in RIS or the drug vehicle were generated as previously described [23]. Briefly, SH-SY5Y cells (pass 13) were cultured in Dulbecco's modified Eagle medium supplemented with 10% (*v/v*) fetal bovine serum and either 100 nM RIS in dimethyl sulfoxide (DMSO) or DMSO alone. Total RNA was extracted and sequenced using the Illumina HiSeq platform. DE traits were identified with a threshold of log-fold change of 1.5 and a significance cutoff of $p < 0.05$. We accessed the DE dataset from entry GSE149611 in the NCBI GEO Database [27,28].

2.3. Transcriptomic Changes Induced by Onset of Aripiprazole Treatment in Psychiatric Patients

Transcriptional changes induced by aripiprazole (ARIP) treatment at first episode of psychosis were previously reported. Briefly, a randomized, flexible-dose, open-label study conducted at University Hospital Marques de Valdecilla, Santander (Spain) collected venous blood draws at patient intake and after three months of treatment with ARIP (5–30 mg/day) [29]. Total RNA was extracted and sequenced using the Illumina HiSeq platform. DE traits were identified by pairwise comparison of baseline transcriptomes to transcriptomes after 3 months of ARIP treatment using Student's *t* test and using a significance cutoff of $p < 0.05$. We accessed the DE dataset from Supplementary Table S2, Crespo-Facorro et al. [30].

2.4. Compilation of Multi-Omic DE Traits

Four lists of DE traits were compiled from the assembled datasets: (1) DE traits in mice treated with OLAN (O_M); (2) DE traits in mice treated with RIS (R_M); (3) DE traits in human cells exposed to RIS (R_H); (4) DE traits in psychiatric patients treated with ARIP (A_H). Lists were examined for functional overlap among DE traits by pairing different subunits of multimeric proteins, identifying receptor/ligand pairs and identifying homologs and paralogs. DE traits that were common to more than one dataset were placed in distinct categories representing all factorial combinations as follows: O_MR_M , O_MR_H , O_MA_H , R_MR_H , R_MA_H , R_HA_H , $O_MR_MR_H$, $O_MR_MA_H$, $R_MR_HA_H$ and $O_MR_MR_HA_H$.

2.5. Pathway Analysis to Detect Alterations in Traits Associated with NAFLD

The Database for Annotation, Visualization and Integrated Discovery (DAVID) v6.8 (<https://david.ncifcrf.gov/home.jsp> (accessed on 20 February 2022)) was used to query the Kyoto Encyclopedia of Genes and Genomes (KEGG) (<https://www.genome.jp/kegg> (accessed on 20 February 2022)) and Genetic Association Database (GAD) Disease databases with all 14 lists of DE traits and to assess involvement in the development of NAFLD [31–34]. Database accessions via DAVID occurred January 2022. Both the Functional Clustering and Functional Annotation Table tools were utilized. NAFLD, Inflammation, Cirrhosis, Obesity, Serum Lipid Levels, Body Mass Index, Lipid Metabolism, Bile Synthesis/Choline Secretion, Waist Circumference, Chronic Hepatitis and Thrombosis were identified as output categories and pathways significantly associated with the pathophysiology of NAFLD. Search terms allowing binning into each pathway are noted in Supplementary Table S1.

2.6. Pathway Analysis to Detect Alterations in Traits Associated with Iron Homeostasis

DAVID was also used to query the KEGG and GAD_Disease databases with each distinct list of DE traits to assess impacts on iron homeostasis. Iron, Hemoglobin, Hemochromatosis, Anemia, Iron Metabolism, Thalassemia and Blood Values were identified as output categories and pathways associated with iron homeostasis. Search terms allowing binning into each pathway are noted in Supplementary Table S2. Mechanistic figures depicting proposed changes in iron transport were generated using BioRender (www.BioRender.com (accessed on 20 February 2022)).

2.7. Measurement of Iron Accumulation in Livers of OLAN-Treated Mice

Iron species in livers from male mice treated with either VEH ($n = 4$) or OLAN ($n = 5$) for 28 days were analyzed for the presence of total iron (Fe), ferrous iron (Fe^{2+}) or ferric iron (Fe^{3+}) using a colorimetric iron assay (Iron assay kit #MAK025 Sigma Aldrich, St Louis, MO, USA). Briefly, a portion of liver (70–192 mg) from each animal was homogenized in assay buffer and adjusted to a final concentration of 250 mg/mL as determined by BCA protein assay (Novagen®Sigma-Aldrich, Saint Louis, MO, USA). These homogenates were centrifuged at $16,000 \times g$ for 10 minutes at 4 °C. The resulting supernatant (25 μL) was processed according to the manufacturer's instructions. Absorbance was determined at 592 nm, and concentration of iron species was interpolated from a standard curve (2.00–10.0 nM) constructed from ferrous, ferric and total iron standards.

3. Results

3.1. Parameters of Subjects Assessed for Differential Expression Induced by Atypical Antipsychotic Drugs

Mice treated for four weeks with low-dose OLAN or RIS did not experience treatment effects on body weight, and all measured vital signs did not differ significantly between drug-treated animals and drug vehicle-treated control animals [7,16]. NAFLD was confirmed in OLAN and RIS mice by histological evaluation [7]. Psychiatric patients treated with ARIP had significantly elevated levels of serum prolactin and 23.6% experienced weight gain, as reported in a separate analysis of the same patient cohort [29]. Twenty-four-hour exposure of SH-SY5Y cells to 100 nM RIS did not result in cytotoxicity [27].

3.2. Multi-omic Analysis Predicts Impacts on NAFLD Development Following Atypical Antipsychotic Drug Exposure In Vitro and In Vivo

Pathway analysis utilizing both the KEGG and GAD_Disease Databases identified numerous DE traits associated with NAFLD or mechanistically associated clinical states. DE traits common to all factorial combinations of AAs and study systems were observed, as were DE traits unique to each dataset. Supplementary Table S3 lists DE traits by dataset combinations and NAFLD-associated pathway. There were 85 NAFLD-associated DE traits common to human cells in vitro and human patients in vivo (Figure 2A), and 35 traits common to RIS exposure in vitro or in vivo (Figure 2B). Only 3 DE traits were found in all

in vivo datasets and none in the in vitro (Figure 2C), whereas 40 NAFLD-associated DE traits were found across all four datasets (Figure 2D).

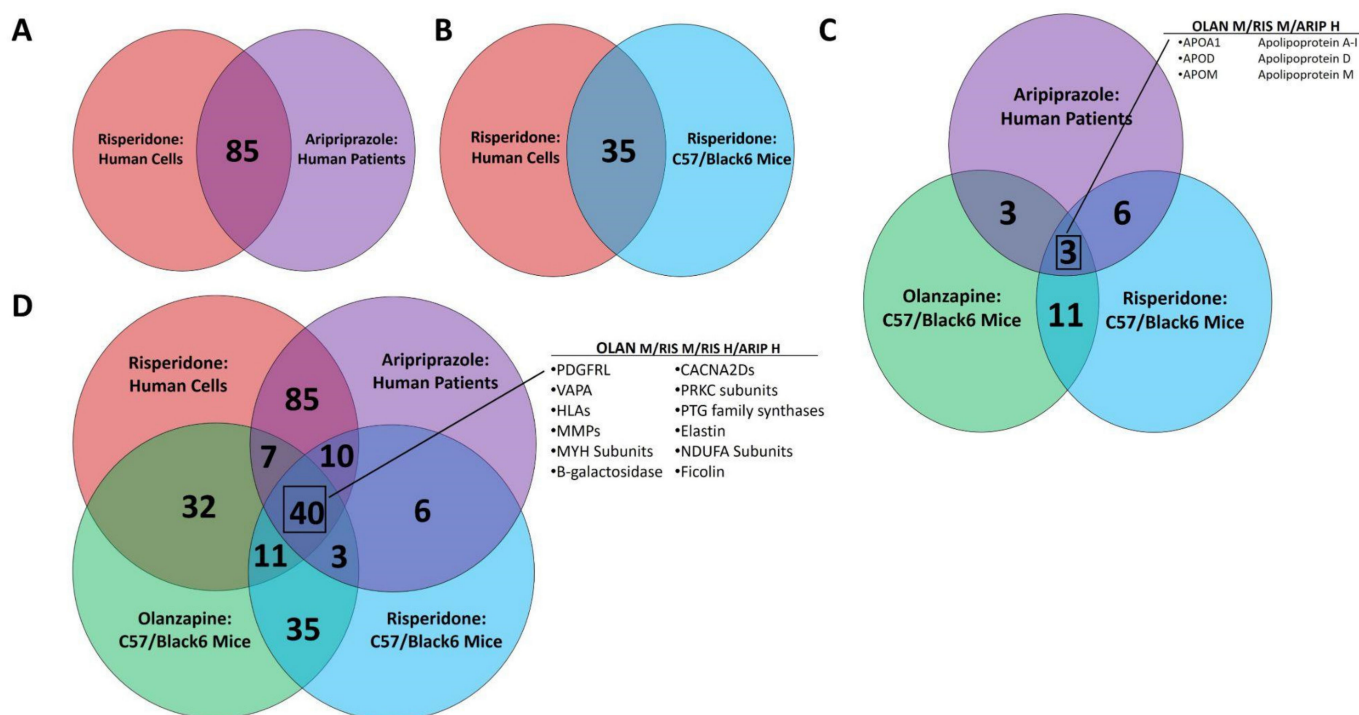


Figure 2. Differentially Expressed Traits Commonly Associated with NAFLD. Venn diagrams representing overlap between AA-exposed multi-omic datasets were generated. Transcriptomic changes in psychiatric patients treated with ARIP are shown in pink, and in human neuroblastoma cells exposed to RIS are shown in purple. Proteomic changes in non-obese mice treated with OLAN are shown in green, and in those treated with RIS are shown in blue. Common changes in human systems in vitro or in vivo are shown, (A) as are common changes induced by RIS in vitro and in vivo. (B) The number of changes seen in vivo that are not seen in vitro are shown (C). DE traits common across study systems are shown in Panel (D), and those of notable interest are listed.

3.3. Multi-omic Analysis Predicts Impacts on Iron Homeostasis following Atypical Antipsychotic Drug Exposure In Vitro and In Vivo

Pathway analysis utilizing both the KEGG and GAD_Disease Databases identified numerous DE traits associated with iron homeostasis and anemia. Supplementary Table S4 lists DE traits by dataset combinations and iron-associated pathway. There were 19 iron-associated DE traits common to human cells in vitro and human patients in vivo (Figure 3A), and 4 traits common to RIS exposure in vitro or in vivo (Figure 3B). A single DE trait, alipoprotein-1A, was found in all in vivo datasets and none were found in vitro (Figure 3C), whereas 7 iron-associated DE traits were found across all four datasets (Figure 3D). Traits unique to each dataset are noted in Figure 3E. The number of DE traits falling within GAD_Disease Database categories for anemia measures (i.e., hemoglobin, hematocrit, erythrocyte count and mean corpuscular volume) are shown for each in vivo system (Figure 4A). The direction of multiple DE traits led the authors to develop a proposed mechanism for the development of clinical anemia following AA exposure (Figure 4B).

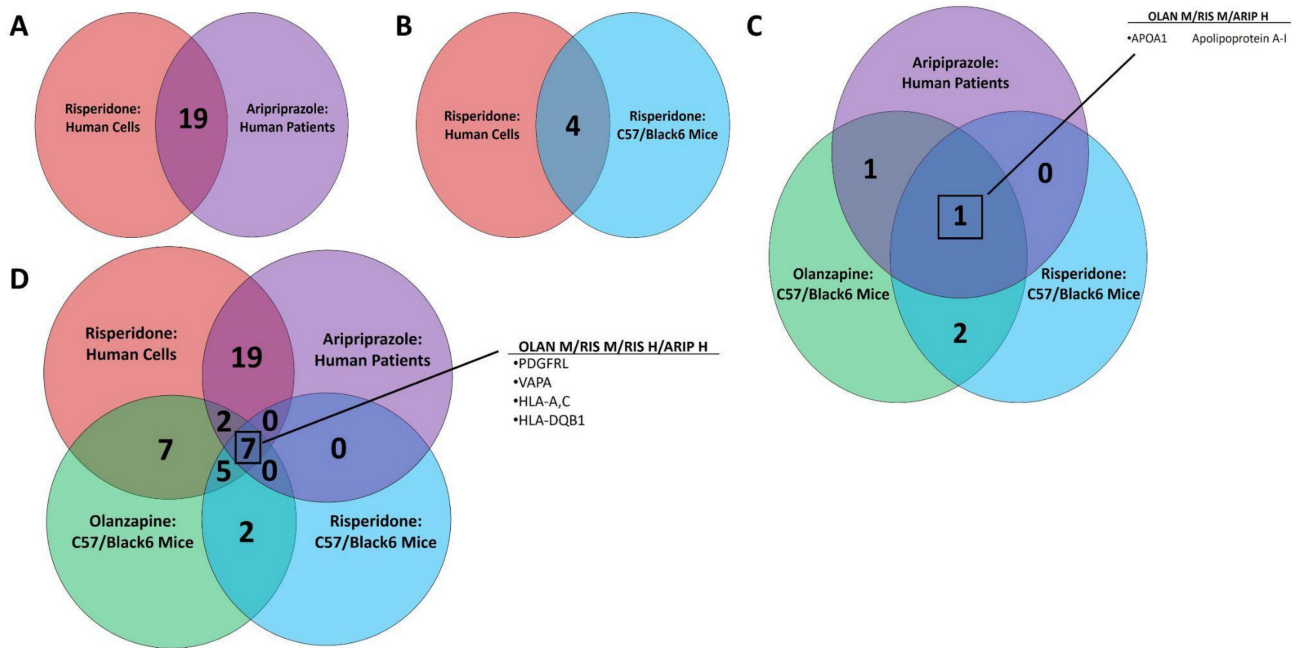


Figure 3. Common Iron-Associated Differentially Expressed Traits. Venn diagrams representing overlap in DE traits related to iron homeostasis between AA-exposed multi-omic data sets were generated. Transcriptomic changes in psychiatric patients treated with ARIP are shown in pink, and in human neuroblastoma cells exposed to RIS are shown in purple. Proteomic changes in non-obese mice treated with OLAN are shown in green, and in non-obese mice treated with RIS are shown in blue. Common changes in human systems in vitro or in vivo are shown, (A) as are common changes induced by RIS in vitro and in vivo. (B) The number of changes seen in vivo that are not seen in vitro are shown. (C) DE traits common across study systems are shown in Panel (D), and the most critical traits are noted.

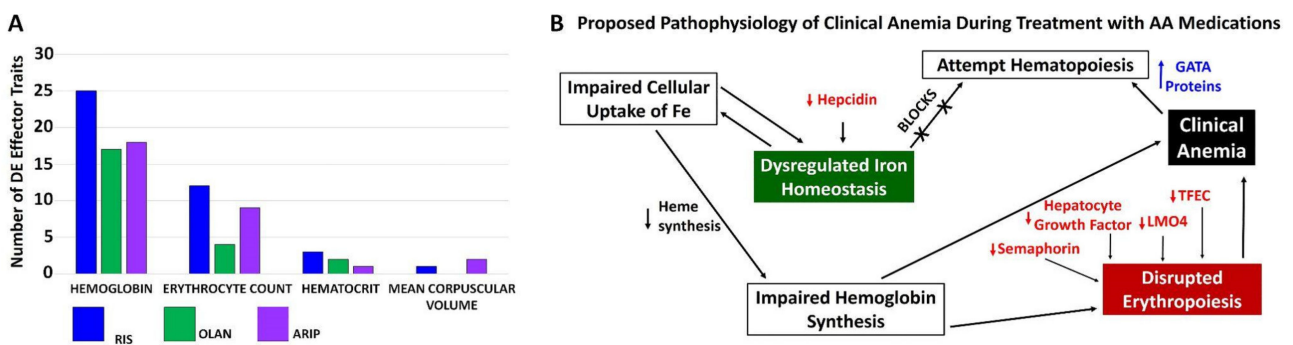


Figure 4. Differentially Expressed Traits In Vivo and Development of Clinical Anemia. Total numbers of DE traits associated with clinical measures of anemia (hemoglobin, hematocrit, erythrocyte count and mean corpuscular volume) in mice treated with RIS (panel (A), blue bars), mice treated with OLAN (panel (A), green bars) and patients treated with ARIP (panel (A), purple bars) are shown. The directional change of multiple DE traits led to the development of a proposed mechanism for the development of clinical anemia following AA exposure (B).

3.4. Proposed Mechanisms of Altered Iron Homeostasis Following Pathway Analysis of Traits Differentially Expressed by Atypical Antipsychotic Drugs

Pathway analysis utilizing both the KEGG and GAD_Disease Databases identified numerous DE traits associated with iron homeostasis. The directional change of multiple DE traits led to the development of a proposed mechanism for altered cellular iron uptake following AA exposure, and how this impairment predicts reduction in circulating ferritin and accumulation of iron in tissues (Figure 5).

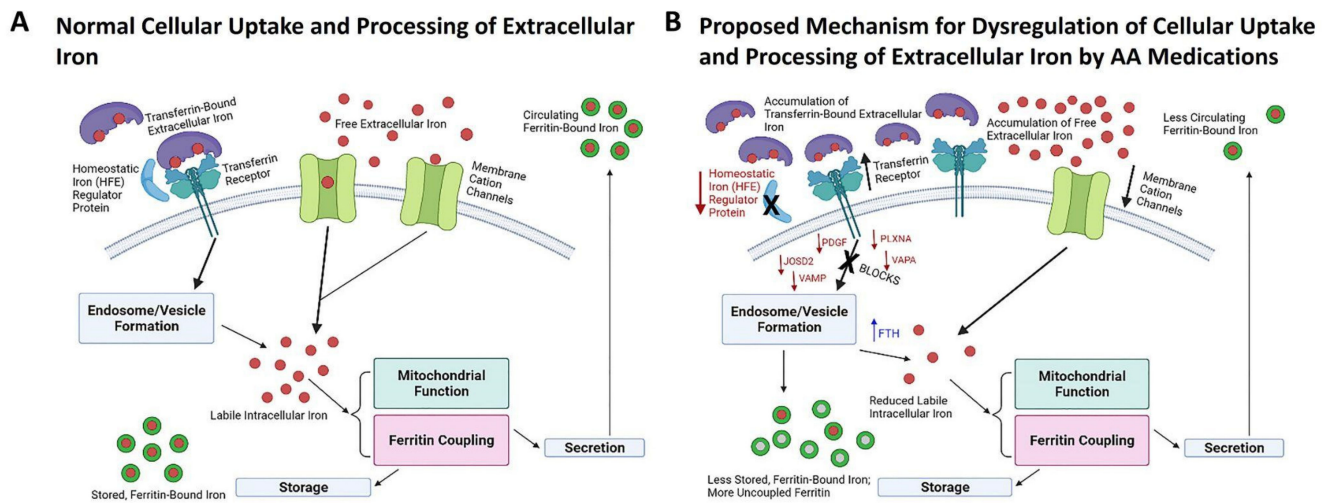


Figure 5. Proposed Mechanism for Impaired Cellular Iron Uptake Based on Differentially Expressed Traits. Panel (A) schematically describes processes for cellular iron uptake, storage and secretion into the circulatory system under physiologically normal conditions. AA-induced decreases of membrane cation channels, the transferrin co-receptor HFE and numerous proteins involved in endosome and vesicle formation suggests an inability to efficiently transport iron into cells and result in accumulation of extracellular iron in the liver (Panel (B)). The reduction in intracellular iron would impair mitochondrial function and reduce the amount of available ferritin-bound iron within cells and in circulation.

3.5. Measurement of Accumulated Iron in Mice Treated with OLAN

In order to test our hypothesis that AA-associated NAFLD is due, at least in part, to drug-induced changes in iron homeostasis, we quantified the concentration of iron species in livers collected from male mice treated sub-chronically with OLAN (Figure 6). We previously reported that these mice developed drug-associated lean NAFLD as determined by histological evaluation [7]. Clinically relevant exposure of AA caused a significant ($p < 0.009$) increase in total Fe concentrations in the liver consistent with gene expression changes in pathways associated with regulation of iron homeostasis coincident with NAFLD.

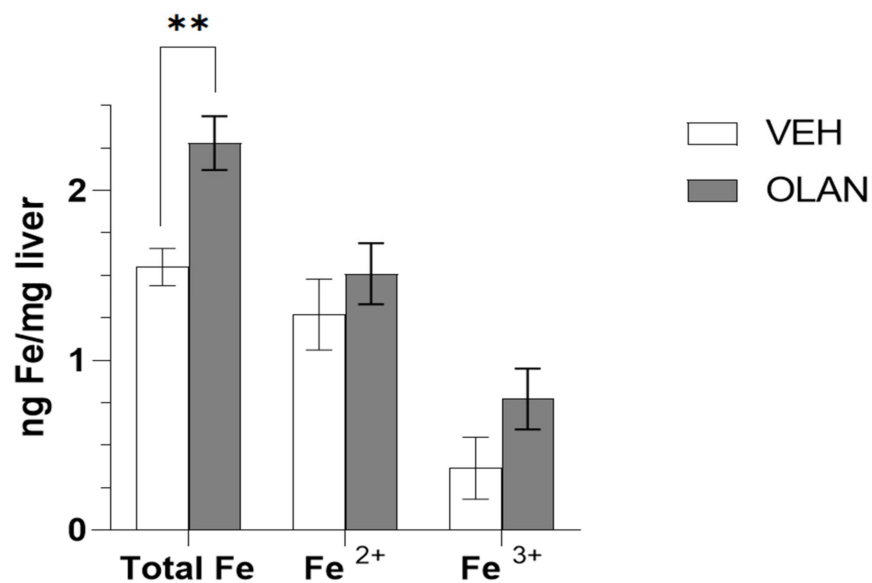


Figure 6. Iron (Fe) concentration in livers of mice treated with vehicle (VEH) or olanzapine (OLAN). Concentrations of iron species were determined in mice treated with VEH ($n = 4$) or OLAN ($n = 5$) daily for 28 days (5 mg/kg OLAN). ** $p < 0.009$.

3.6. Proposed Mechanisms of NAFLD Development Following Pathway Analysis of Traits Differentially Expressed by Atypical Antipsychotic Drugs

Pathway analysis utilizing both the KEGG and GAD_Disease Databases identified numerous DE traits associated with NAFLD and iron homeostasis. The directional change of multiple DE traits led to the development of a proposed mechanism for AA-induced NAFLD (Figure 7).

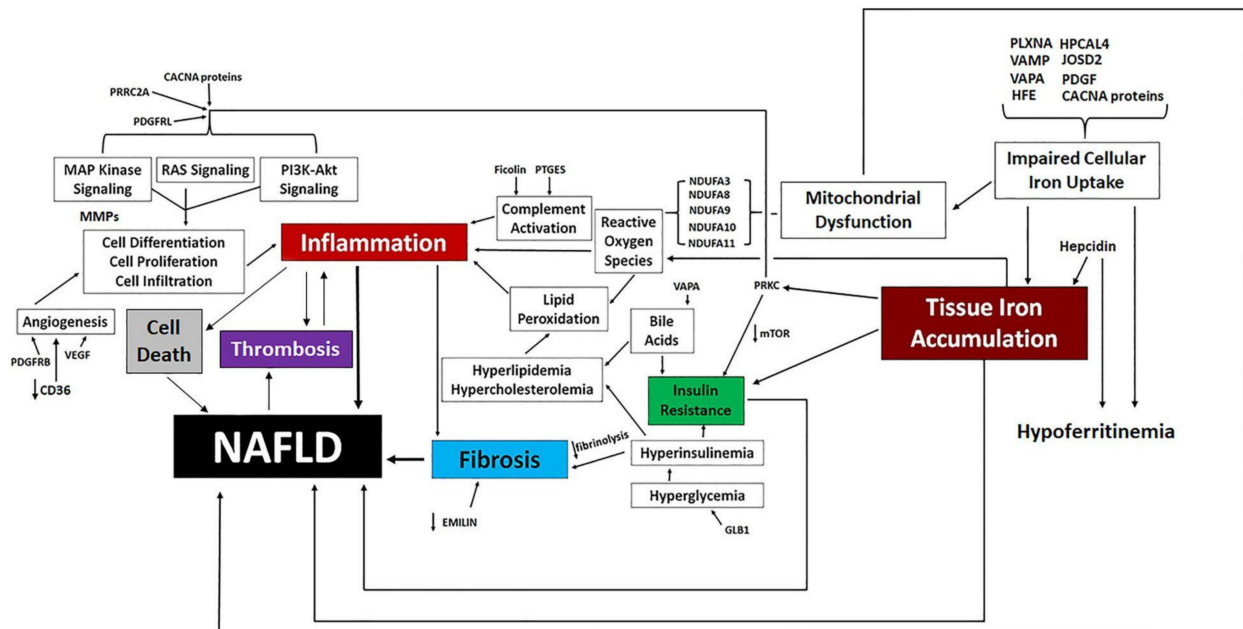


Figure 7. Proposed Molecular Mechanisms Underlying the Clinical Development of AA-Induced NAFLD.

4. Discussion

Development of NAFLD has been associated with AA treatment in preclinical models and patient populations [35–38], and patients treated with AA medications have been reported to have significantly higher rates of iron-deficiency anemia [17,26,39–44] and obesity [12–15]. Despite these reports, pathophysiological mechanisms by which AA treatment can lead to NAFLD and disruptions in iron homeostasis remain virtually unexplored. We combined multi-omic data sets utilizing three different AA medications, one in vitro model system, two in vivo preclinical model systems and one patient cohort to identify commonalities across drugs and study systems in order to propose potential mechanisms leading to these complications that can be prospectively evaluated in future studies wherein changes to specific traits are measured. Whereas NAFLD could only be histologically confirmed in the two preclinical models, the inclusion of data from subjects with and without drug-associated increase in body weight (i.e., lean preclinical animals and a patient cohort with reported weight gain at 3 months of drug treatment) indicates that the data from the in vivo systems represent a spectrum of AA-induced metabolic effects. Importantly, our multi-omic approach provided preliminary evidence that drug effects on metabolic dysregulation as observed in NAFLD is translational across the drug class and across species and model systems. Furthermore, dysregulation of gene and protein expression in NAFLD-associated pathways occurs at the cellular and organismal level, in the presence and absence of obesity and with acute and subchronic treatment duration. We note that NAFLD was only histologically confirmed in pre-clinical models, and mechanistic overlap with in vitro and in vivo gene expression changes should be considered supportive of mechanistic hypotheses rather than trans-species evidence of proposed mechanisms. Prospective evaluations of potential biomarkers in humans require further evaluation. However, screening guidelines for NAFLD recently released by the American Association of Clinical Endocrinology recommend calculation of a fibrosis-4 (FIB-4) index for high-risk

patients [45] in primary care or endocrinology outpatient settings. This is noteworthy as platelet levels are a crucial component of FIB-4 index calculations, and our omic data-driven mechanistic hypotheses predict changes to risk of thrombosis as shown by DE of 15 thrombosis-related traits across all datasets (Table S3).

The liver plays a central role in the regulation of whole-body iron homeostasis, and chronic liver diseases such as NAFLD and NASH are associated with disruption in iron metabolism [46,47]. Reduced liver function in NAFLD/NASH can lead to hepatic iron overload, culminating in oxidative stress and iron-associated cellular damage [48]. Here, we report that three AA medications alter multiple pathways implicated in the regulation of iron metabolism across model systems, and in the presumed presence (psychiatric patients) or absence (mice) of obesity. We confirm AA treatment altered total hepatic iron content in the livers from mice treated with OLAN (Figure 6) with coincident histological evidence of NAFLD as previously published [7]. The relationship between NAFLD, hemoglobin levels and erythrocyte count is becoming increasingly appreciated to the extent that both erythrocyte count and hemoglobin level have been proposed as potential biomarkers for NAFLD [49,50].

Our proposed model of impaired iron transport (Figure 5) involves a decrease in cation channels (CACNA proteins), decreased transferrin co-receptor HFE and impaired vesicle formation indicating a reduction in cellular iron and an accumulation of extracellular iron. Whereas CACNA proteins were originally described as calcium channels, they have been strongly implicated in iron transport as well [51]. The reduction of intracellular iron leads to impairment of mitochondrial function and decreased ferritin-coupled iron. We and others have reported AA-associated mitochondrial dysfunction as an underlying cause of AA-associated metabolic side effects [16,52]. Hypoferritinemia and/or iron-deficiency anemia has also been reported for patients treated with risperidone [21,26,39,40]. Additionally, chronic treatment (12 weeks) of rats with the AA medication clozapine or the first generation (typical) antipsychotic medication haloperidol resulted in sex-dependent effects on hepatic iron metabolism and anemia [53]. Sudden-onset anemia associated with clozapine and lurasidone that resolves upon cessation of treatment has also been described in case reports [41,42]. These data, which were generated using antipsychotic medications with distinct pharmacology from the AA drugs we report, are nevertheless consistent with our findings for effects of the atypical antipsychotic drugs olanzapine, risperidone and aripiprazole on hepatic iron metabolism. Taken together, these findings support our hypothesis mechanistically linking disrupted iron homeostasis, AA-induced anemia and NAFLD to AA medications. Future prospective testing of these hypotheses will be critical to the development of biomarkers for the clinical evaluation of NAFLD in addition to screening by FIB-4 index.

5. Conclusions

Incidence of NAFLD is increased in patients with psychiatric illness, and antipsychotic medications independently increase NAFLD risk. AAs are widely prescribed to treat a variety of psychiatric disorders and the increase in their off-label use has raised reasonable concerns regarding their significant metabolic side effects. In this paper, we employed a multi-omic, mechanistic approach to better understand the mechanistic pharmacology of AA-induced metabolic disease, including NAFLD and anemia. We found AA-associated dysregulation of NAFLD-associated pathways linking insulin resistance, inflammation, mitochondrial dysfunction and altered iron metabolism in the absence and presence of drug-associated weight gain. These novel findings highlight the significant impact of AA medications on metabolic burden and the need for holistic patient monitoring beyond a focus on weight gain. Clinical guidelines for metabolic monitoring of patients taking AA should be closely followed, especially in vulnerable patient populations, including children [54]. Specifically, monitoring baseline and sustained bodyweight, waist circumference, blood pressure and biomarkers relating to glycemia, lipids and liver function (enzymes),

and changes to FIB-4 index are recommended. Clinical monitoring guidelines specifically focused on NAFLD/NASH in psychiatry have not yet been developed.

Supplementary Materials: The following supporting information can be downloaded at: <https://www.mdpi.com/article/10.3390/biomedicines10061225/s1>, Supplementary Table S1: Binning Terms for NAFLD-Associated Pathways; Supplementary Table S2: Binning Terms for Iron Homeostasis-Associated Pathways; Supplementary Table S3: DE Traits from NAFLD-Associated Pathways; Supplementary Table S4: DE Traits from Iron-Associated Pathways.

Author Contributions: Conceptualization, K.L.H. and M.M.; methodology, M.M., D.B. and K.L.H.; validation, K.L.H. and M.M.; formal analysis, M.M., D.B. and K.L.H.; investigation, M.M., D.B. and K.L.H.; resources, K.L.H. and M.M.; data curation, M.M. and K.L.H.; writing—original draft preparation, M.M., R.I. and K.L.H.; writing—review and editing, M.M., R.I. and K.L.H.; visualization, M.M. and K.L.H.; supervision, M.M. and K.L.H.; project administration, K.L.H.; funding acquisition, K.L.H. All authors have read and agreed to the published version of the manuscript.

Funding: This work was supported by the National Institutes of Health, NIDDK award number DK095143 to KLH.

Institutional Review Board Statement: The University of New England’s Institutional Review Board reviewed our request to access data from de-identified patient samples collected before and after ARIP treatment. The committee formally exempted this analysis (UNE IRB #1221–18).

Informed Consent Statement: Informed consent was obtained from psychiatric patients before and after onset of ARIP treatment by the study authors as previously described [49].

Data Availability Statement: Original datasets are available as described in [7,9,12,23,25] and as noted in the Methods. Complete lists of DE traits commonly expressed between groups can be found at (DOI: 10.13140/RG.2.2.20998.65601).

Conflicts of Interest: The authors declare no conflict of interest.

References

1. Germani, G.; Becchetti, C. Liver transplantation for non-alcoholic fatty liver disease. *Minerva Gastroenterol. Dietol.* **2018**, *64*, 138–146. [[CrossRef](#)] [[PubMed](#)]
2. Benedict, M.; Zhang, X. Non-Alcoholic Fatty Liver Disease: An Expanded Review. *World J. Hepatol.* **2017**, *9*, 715–732. [[CrossRef](#)] [[PubMed](#)]
3. Stefan, N.; Cusi, K. A global view of the interplay between non-alcoholic fatty liver disease and diabetes. *Lancet Diabetes Endocrinol.* **2022**, *10*, 284–296. [[CrossRef](#)]
4. Anstee, Q.M.; Targher, G.; Day, C.P. Progression of NAFLD to diabetes mellitus, cardiovascular disease or cirrhosis. *Nat. Rev. Gastroenterol. Hepatol.* **2013**, *10*, 330–344. [[CrossRef](#)] [[PubMed](#)]
5. Colognesi, M.; Gabbia, D.; De Martin, S. Depression and Cognitive Impairment—Extrahepatic Manifestations of NAFLD and NASH. *Biomedicines* **2020**, *8*, 229. [[CrossRef](#)]
6. Soto-Angona, Ó.; Anmella, G.; Valdés-Flrido, M.J.; De Uribe-Viloria, N.; Carvalho, A.F.; Penninx, B.W.J.H.; Berk, M. Non-alcoholic fatty liver disease (NAFLD) as a neglected metabolic companion of psychiatric disorders: Common pathways and future approaches. *BMC Med.* **2020**, *18*, 261. [[CrossRef](#)]
7. Rostama, B.; Beauchemin, M.; Bouchard, C.; Bernier, E.; Vary, C.P.; May, M.; Houseknecht, K.L. Understanding Mechanisms Underlying Non-Alcoholic Fatty Liver Disease (NAFLD) in Mental Illness: Risperidone and Olanzapine Alter the Hepatic Proteomic Signature in Mice. *Int. J. Mol. Sci.* **2020**, *21*, 9362. [[CrossRef](#)]
8. Xu, H.; Zhuang, X. Atypical antipsychotics-induced metabolic syndrome and nonalcoholic fatty liver disease: A critical review. *Neuropsychiatr. Dis. Treat.* **2019**, *15*, 2087–2099. [[CrossRef](#)]
9. May, M.; Beauchemin, M.; Vary, C.; Barlow, D.; Houseknecht, K.L. The antipsychotic medication, risperidone, causes global immunosuppression in healthy mice. *PLoS ONE* **2019**, *14*, e0218937. [[CrossRef](#)]
10. Freyberg, Z.; Aslanoglou, D.; Shah, R.; Ballon, J.S. Intrinsic and Antipsychotic Drug-Induced Metabolic Dysfunction in Schizophrenia. *Front. Neurosci.* **2017**, *11*, 432. [[CrossRef](#)]
11. Bauer, M.E.; Teixeira, A.L. Inflammation in psychiatric disorders: What comes first? *Ann. N. Y. Acad. Sci. USA* **2019**, *1437*, 57–67. [[CrossRef](#)]
12. Alvarez-Jiménez, M.; González-Blanch, C.; Crespo-Facorro, B.; Hetrick, S.; Rodríguez-Sánchez, J.M.; Pérez-Iglesias, R.; Vázquez-Barquero, J.L. Antipsychotic-Induced Weight Gain in Chronic and First-Episode Psychotic Disorders: A Systematic Critical Reappraisal. *CNS Drugs* **2008**, *22*, 547–562. [[CrossRef](#)]

13. Pillinger, T.; McCutcheon, R.A.; Vano, L.; Mizuno, Y.; Arumuham, A.; Hindley, G.; Beck, K.; Natesan, S.; Efthimiou, O.; Cipriani, A.; et al. Comparative Effects of 18 Antipsychotics on Metabolic Function in Patients with Schizophrenia, Predictors of Metabolic Dysregulation, and Association with Psychopathology: A Systematic Review and Network Meta-Analysis. *Lancet Psychiatry* **2020**, *7*, 64–77. [[CrossRef](#)]
14. Zipursky, R.B.; Gu, H.; Green, A.I.; Perkins, D.O.; Tohen, M.F.; McEvoy, J.P.; Strakowski, S.M.; Sharma, T.; Kahn, R.S.; Gur, R.E.; et al. Course and Predictors of Weight Gain in People with First-Episode Psychosis Treated with Olanzapine or Haloperidol. *Br. J. Psychiatry* **2005**, *187*, 537–543. [[CrossRef](#)]
15. Annamalai, A.; Kosir, U.; Tek, C. Prevalence of Obesity and Diabetes in Patients with Schizophrenia. *World J. Diabetes* **2017**, *15*, 390–396. [[CrossRef](#)]
16. Beauchemin, M.; Geguchadze, R.; Guntur, A.R.; Nevola, K.; Le, P.T.; Barlow, D.; Rue, M.; Vary, C.P.H.; Lary, C.W.; Motyl, K.J.; et al. Exploring mechanisms of increased cardiovascular disease risk with antipsychotic medications: Risperidone alters the cardiac proteomic signature in mice. *Pharmacol. Res.* **2020**, *152*, 104589. [[CrossRef](#)]
17. Houseknecht, K.L.; Robertson, A.S.; Zavadski, W.; Gibbs, E.M.; Johnson, D.E.; Rollema, H. Acute effects of atypical antipsychotics on whole-body insulin resistance in rats: Implications for adverse metabolic effects. *Neuropsychopharmacology* **2007**, *32*, 289–297. [[CrossRef](#)]
18. Dongiovanni, P.; Fracanzani, A.L.; Fargion, S.; Valenti, L. Iron in fatty liver and in the metabolic syndrome: A promising therapeutic target. *J. Hepatol.* **2011**, *55*, 920–932. [[CrossRef](#)]
19. Marmur, J.; Beshara, S.; Eggertsen, G.; Onelöv, L.; Albiin, N.; Danielsson, O.; Hultcrantz, R.; Stål, P. Hepcidin levels correlate to liver iron content, but not steatohepatitis, in non-alcoholic fatty liver disease. *BMC Gastroenterol.* **2018**, *18*, 78. [[CrossRef](#)]
20. McCann, J.C.; Ames, B.N. An overview of evidence for a causal relation between iron deficiency during development and deficits in cognitive or behavioral function. *Am. J. Clin. Nutr.* **2007**, *85*, 931–945. [[CrossRef](#)]
21. Calarge, C.A.; Murry, D.J.; Ziegler, E.E.; Arnold, L.E. Serum Ferritin, Weight Gain, Disruptive Behavior, and Extrapyrmidal Symptoms in Risperidone-Treated Youth. *J. Child Adolesc. Psychopharmacol.* **2016**, *26*, 471–477. [[CrossRef](#)]
22. Grantham-McGregor, S.; Ani, C. A review of studies on the effect of iron deficiency on cognitive development in children. *J. Nutr.* **2001**, *131*, 649S–666S, discussion 666S–668S. [[CrossRef](#)]
23. Nelson, J.E.; Klintworth, H.; Kowdley, K.V. Iron metabolism in Nonalcoholic Fatty Liver Disease. *Curr. Gastroenterol. Rep.* **2012**, *14*, 8–16. [[CrossRef](#)]
24. Schoretsanitis, G.; Nikolakopoulou, A.; Guinart, D.; Correll, C.U.; Kane, J.M. Iron homeostasis alterations and risk for akathisia in patients treated with antipsychotics: A systematic review and meta-analysis of cross-sectional studies. *Eur. Neuropsychopharmacol.* **2020**, *35*, 1–11. [[CrossRef](#)]
25. Chong, S.A.; Mythily, M.B.B.S.; Remington, G. Tardive dyskinesia and iron status. *J. Clin. Psychopharmacol.* **2004**, *24*, 235–236. [[CrossRef](#)]
26. Calarge, C.A.; Ziegler, E.E.; Del Castillo, N.; Aman, M.; McDougle, C.J.; Scahill, L.; McCracken, J.T.; Arnold, L.E. Iron homeostasis during risperidone treatment in children and adolescents. *J. Clin. Psychiatry* **2015**, *76*, 1500–1505. [[CrossRef](#)]
27. Malekizadeh, Y.; Williams, G.; Kelson, M.; Whitfield, D.; Mill, J.; Collier, D.A.; Ballard, C.; Jeffries, A.R.; Creese, B. Whole transcriptome in silico screening implicates cardiovascular and infectious disease in the mechanism of action underlying atypical antipsychotic side effects. *Alzheimers Dement.* **2020**, *6*, e12078. [[CrossRef](#)]
28. Barrett, T.; Wilhite, S.E.; Ledoux, P.; Evangelista, C.; Kim, I.F.; Tomashevsky, M.; Marshall, K.A.; Phillippy, K.H.; Sherman, P.M.; Holko, M.; et al. NCBI GEO: Archive for functional genomics data sets—Update. *Nucleic Acids Res.* **2013**, *41*, D991–D995. [[CrossRef](#)]
29. Crespo-Facorro, B.; Ortiz-Garcia de la Foz, V.; Suarez-Pinilla, P.; Valdizan, E.M.; Pérez-Iglesias, R.; Amado-Señaris, J.A.; Teresa Garcia-Unzueta, M.; Labad, J.; Correll, C.; Ayesa-Arriola, R. Effects of aripiprazole, quetiapine and ziprasidone on plasma prolactin levels in individuals with first episode nonaffective psychosis: Analysis of a randomized open-label 1 year study. *Schizophr. Res.* **2017**, *189*, 134–141. [[CrossRef](#)]
30. Crespo-Facorro, B.; Ruiz-Veguilla, M.; Vázquez-Bourgon, J.; Sánchez-Hidalgo, A.C.; Garrido-Torres, N.; Cisneros, J.M.; Prieto, C.; Sainz, J. Aripiprazole as a Candidate Treatment of COVID-19 Identified Through Genomic Analysis. *Front. Pharmacol.* **2021**, *12*, 646701. [[CrossRef](#)]
31. Huang, D.W.; Sherman, B.T.; Lempicki, R.A. Bioinformatics enrichment tools: Paths toward the comprehensive functional analysis of large gene lists. *Nucleic Acids Res.* **2009**, *37*, 1–13. [[CrossRef](#)] [[PubMed](#)]
32. Huang, D.W.; Sherman, B.T.; Lempicki, R.A. Systematic and integrative analysis of large gene lists using DAVID bioinformatics resources. *Nat. Protoc.* **2009**, *4*, 44–57. [[CrossRef](#)] [[PubMed](#)]
33. Kanehisa, M.; Goto, S. KEGG: Kyoto encyclopedia of genes and genomes. *Nucleic Acids Res.* **2000**, *28*, 27–30. [[CrossRef](#)] [[PubMed](#)]
34. Becker, K.G.; Barnes, K.C.; Bright, T.J.; Wang, S.A. The genetic association database. *Nat. Genet.* **2004**, *36*, 431–432. [[CrossRef](#)]
35. Soliman, H.M.; Wagih, H.M.; Algaidi, S.A.; Hafiz, A.H. Histological evaluation of the role of atypical antipsychotic drugs in inducing non-alcoholic fatty liver disease in adult male albino rats (light and electron microscopic study). *Folia Biol.* **2013**, *59*, 173–180.

36. Morlán-Coarasa, M.J.; Arias-Loste, M.T.; Ortiz-García de la Foz, V.; Martínez-García, O.; Alonso-Martín, C.; Crespo, J.; Romero-Gómez, M.; Fábrega, E.; Crespo-Facorro, B. Incidence of non-alcoholic fatty liver disease and metabolic dysfunction in first episode schizophrenia and related psychotic disorders: A 3-year prospective randomized interventional study. *Psychopharmacology* **2016**, *233*, 3947–3952. [[CrossRef](#)]
37. Koreki, A.; Mori, H.; Nozaki, S.; Koizumi, T.; Suzuki, H.; Onaya, M. Risk of Nonalcoholic Fatty Liver Disease in Patients With Schizophrenia Treated With Antipsychotic Drugs: A Cross-sectional Study. *J. Clin. Psychopharmacol.* **2021**, *41*, 474–477. [[CrossRef](#)]
38. Li, R.; Zhu, W.; Huang, P.; Yang, Y.; Luo, F.; Dai, W.; Shen, L.; Pei, W.; Huang, X. Olanzapine leads to nonalcoholic fatty liver disease through the apolipoprotein A5 pathway. *Biomed. Pharmacother.* **2021**, *141*, 111803. [[CrossRef](#)]
39. Chen, X.; Li, Y.; Zhang, T.; Yao, Y.; Shen, C.; Xue, Y. Association of Serum Trace Elements with Schizophrenia and Effects of Antipsychotic Treatment. *Biol. Trace Elem. Res.* **2018**, *181*, 22–30. [[CrossRef](#)]
40. Calarge, C.A.; Ziegler, E.E. Iron deficiency in pediatric patients in long-term risperidone treatment. *J. Child Adolesc. Psychopharmacol.* **2013**, *23*, 101–109. [[CrossRef](#)]
41. Eleftheriou, G.; Butera, R.; Barcella, L.; Falanga, A. Clozapine-induced anemia: A case-report. *Int. J. Clin. Pharmacol. Ther.* **2020**, *58*, 289–292. [[CrossRef](#)]
42. Kirpekar, V.C.; Faye, A.D.; Bhave, S.H.; Tadke, R.; Gawande, S. Lurasidone-induced anemia: Is there a need for hematological monitoring? *Indian J. Pharmacol.* **2019**, *51*, 276–278.
43. Capeto Coelho, I.; Aleixo, A.; Linhares, L.; Martins, A.; Telles Correia, D. Hemolytic anemia potentially associated with aripiprazole. *Psychiatry Clin. Neurosci.* **2018**, *72*, 876. [[CrossRef](#)]
44. Moulin, V.; Grandoni, F.; Castioni, J.; Lu, H. Pancytopenia in an adult patient with thiamine-responsive megaloblastic anaemia. *BMJ Case Rep.* **2018**, *2018*, bcr-2018. [[CrossRef](#)]
45. Cusi, K.; Isaacs, S.; Barb, D.; Rinella, M.E.; Vos, M.B.; Younossi, Z. American Association of Clinical Endocrinology Clinical Practice Guideline for the Diagnosis and Management of Nonalcoholic Fatty Liver Disease in Primary Care and Endocrinology Clinical Settings Co-Sponsored by the American Association for the Study of Liver Diseases (AASLD). *AACE Endocr. Pract.* **2022**, *28*, 528–562.
46. Milic, S.; Mikolasevic, I.; Orlic, L.; Devcic, E.; Starcevic-Cizmarevic, N.; Stimac, D.; Kapovic, M.; Ristic, S. The Role of Iron and Iron Overload in Chronic Liver Disease. *Med. Sci. Monit.* **2016**, *22*, 2144–2151. [[CrossRef](#)]
47. Datz, C.; Müller, E.; Aigner, E. Iron overload and non-alcoholic fatty liver disease. *Minerva Endocrinol.* **2017**, *42*, 173–183. [[CrossRef](#)]
48. Masarone, M.; Rosato, V.; Dallio, M.; Gravina, A.G.; Aglitti, A.; Loguercio, C.; Federico, A.; Persico, M. Role of Oxidative Stress in Pathophysiology of Nonalcoholic Fatty Liver Disease. *Oxid. Med. Cell. Longev.* **2018**, *2018*, 9547613. [[CrossRef](#)]
49. Zhong, F.; Guan, L.; Lin, H.; Zhao, M.; Qin, Y.; Li, Q.; Yuan, Z.; Yang, G.; Gao, L.; Zhao, J. Red Blood Cell Count: An Unrecognized Risk Factor for Nonalcoholic Fatty Liver Disease. *Front. Endocrinol.* **2021**, *12*, 760981. [[CrossRef](#)]
50. Jiang, Y.; Zeng, J.; Chen, B. Hemoglobin combined with triglyceride and ferritin in predicting non-alcoholic fatty liver. *J. Gastroenterol. Hepatol.* **2014**, *29*, 1508–1514. [[CrossRef](#)]
51. Oudit, G.Y.; Trivieri, M.G.; Khaper, N.; Liu, P.P.; Backx, P.H. Role of L-type Ca²⁺ channels in iron transport and iron-overload cardiomyopathy. *J. Mol. Med.* **2006**, *84*, 349–364. [[CrossRef](#)]
52. Del Campo, A.; Bustos, C.; Mascayano, C.; Acuña-Castillo, C.; Troncoso, R.; Rojo, L.E. Metabolic Syndrome and Antipsychotics: The Role of Mitochondrial Fission/Fusion Imbalance. *Front. Endocrinol.* **2018**, *9*, 144. [[CrossRef](#)]
53. Bouvier, M.L.; Fehsel, K.; Schmitt, A.; Meisenzahl-Lechner, E.; Gaebel, W.; Von Wilmsdorff, M. Sex-dependent effects of long-term clozapine or haloperidol medication on red blood cells and liver iron metabolism in Sprague Dawley rats as a model of metabolic syndrome. *BMC Pharmacol. Toxicol.* **2022**, *23*, 8. [[CrossRef](#)]
54. American Diabetes Association; American Psychiatric Association; American Association of Clinical Endocrinologists; North American Association for the Study of Obesity. Consensus Development Conference on Antipsychotic Drugs and Obesity and Diabetes. *J. Clin. Psychiatry* **2004**, *65*, 267–272. [[CrossRef](#)]